BABAR-CONF-02/19
SLAC-PUB-9322
July 2002

Measurement of the Branching Fractions for the Exclusive Decays of B^0 and B^+ to $\overline{D}^{(*)}D^{(*)}K$

The *BABAR* Collaboration

July 26, 2002

Abstract

Using data collected with the *BABAR* detector between 1999 and 2002, we report the observation of 823±57 B^0 and 969±65 B^+ decays to $\overline{D}^{(*)}D^{(*)}K$, where $\overline{D}^{(*)}$ and $D^{(*)}$ are fully reconstructed and where K is either a $K^{\pm}$ or a K^0_S decaying to $\pi^+\pi^-$. All 22 possible B decays to $\overline{D}^{(*)}D^{(*)}K$ are reconstructed exclusively and the corresponding branching fractions or limits are determined. The preliminary branching fractions of the B^0 and of the B^+ to $\overline{D}^{(*)}D^{(*)}K$ are found to be

$$\mathcal{B}(B^0 \to \overline{D}^{(*)}D^{(*)}K) = (4.3 \pm 0.3(stat) \pm 0.6(syst)) \times 10^{-2},$$
$$\mathcal{B}(B^+ \to \overline{D}^{(*)}D^{(*)}K) = (3.5 \pm 0.3(stat) \pm 0.5(syst)) \times 10^{-2}.$$

Contributed to the 31^{st} International Conference on High Energy Physics,
7/24—7/31/2002, Amsterdam, The Netherlands

Stanford Linear Accelerator Center, Stanford University, Stanford, CA 94309

Work supported in part by Department of Energy contract DE-AC03-76SF00515.

The *BABAR* Collaboration,

B. Aubert, D. Boutigny, J.-M. Gaillard, A. Hicheur, Y. Karyotakis, J. P. Lees, P. Robbe, V. Tisserand, A. Zghiche

Laboratoire de Physique des Particules, F-74941 Annecy-le-Vieux, France

A. Palano, A. Pompili

Università di Bari, Dipartimento di Fisica and INFN, I-70126 Bari, Italy

J. C. Chen, N. D. Qi, G. Rong, P. Wang, Y. S. Zhu

Institute of High Energy Physics, Beijing 100039, China

G. Eigen, I. Ofte, B. Stugu

University of Bergen, Inst. of Physics, N-5007 Bergen, Norway

G. S. Abrams, A. W. Borgland, A. B. Breon, D. N. Brown, J. Button-Shafer, R. N. Cahn, E. Charles, M. S. Gill, A. V. Gritsan, Y. Groysman, R. G. Jacobsen, R. W. Kadel, J. Kadyk, L. T. Kerth, Yu. G. Kolomensky, J. F. Kral, C. LeClerc, M. E. Levi, G. Lynch, L. M. Mir, P. J. Oddone, T. J. Orimoto, M. Pripstein, N. A. Roe, A. Romosan, M. T. Ronan, V. G. Shelkov, A. V. Telnov, W. A. Wenzel

Lawrence Berkeley National Laboratory and University of California, Berkeley, CA 94720, USA

T. J. Harrison, C. M. Hawkes, D. J. Knowles, S. W. O'Neale, R. C. Penny, A. T. Watson, N. K. Watson

University of Birmingham, Birmingham, B15 2TT, United Kingdom

T. Deppermann, K. Goetzen, H. Koch, B. Lewandowski, K. Peters, H. Schmuecker, M. Steinke

Ruhr Universität Bochum, Institut für Experimentalphysik 1, D-44780 Bochum, Germany

N. R. Barlow, W. Bhimji, J. T. Boyd, N. Chevalier, P. J. Clark, W. N. Cottingham, C. Mackay, F. F. Wilson

University of Bristol, Bristol BS8 1TL, United Kingdom

K. Abe, C. Hearty, T. S. Mattison, J. A. McKenna, D. Thiessen

University of British Columbia, Vancouver, BC, Canada V6T 1Z1

S. Jolly, A. K. McKemey

Brunel University, Uxbridge, Middlesex UB8 3PH, United Kingdom

V. E. Blinov, A. D. Bukin, A. R. Buzykaev, V. B. Golubev, V. N. Ivanchenko, A. A. Korol, E. A. Kravchenko, A. P. Onuchin, S. I. Serednyakov, Yu. I. Skovpen, A. N. Yushkov

Budker Institute of Nuclear Physics, Novosibirsk 630090, Russia

D. Best, M. Chao, D. Kirkby, A. J. Lankford, M. Mandelkern, S. McMahon, D. P. Stoker

University of California at Irvine, Irvine, CA 92697, USA

C. Buchanan, S. Chun

University of California at Los Angeles, Los Angeles, CA 90024, USA

H. K. Hadavand, E. J. Hill, D. B. MacFarlane, H. Paar, S. Prell, Sh. Rahatlou, G. Raven, U. Schwanke, V. Sharma

University of California at San Diego, La Jolla, CA 92093, USA

J. W. Berryhill, C. Campagnari, B. Dahmes, P. A. Hart, N. Kuznetsova, S. L. Levy, O. Long, A. Lu, M. A. Mazur, J. D. Richman, W. Verkerke

University of California at Santa Barbara, Santa Barbara, CA 93106, USA

J. Beringer, A. M. Eisner, M. Grothe, C. A. Heusch, W. S. Lockman, T. Pulliam, T. Schalk, R. E. Schmitz, B. A. Schumm, A. Seiden, M. Turri, W. Walkowiak, D. C. Williams, M. G. Wilson

University of California at Santa Cruz, Institute for Particle Physics, Santa Cruz, CA 95064, USA

E. Chen, G. P. Dubois-Felsmann, A. Dvoretskii, D. G. Hitlin, F. C. Porter, A. Ryd, A. Samuel, S. Yang

California Institute of Technology, Pasadena, CA 91125, USA

S. Jayatilleke, G. Mancinelli, B. T. Meadows, M. D. Sokoloff

University of Cincinnati, Cincinnati, OH 45221, USA

T. Barillari, P. Bloom, W. T. Ford, U. Nauenberg, A. Olivas, P. Rankin, J. Roy, J. G. Smith, W. C. van Hoek, L. Zhang

University of Colorado, Boulder, CO 80309, USA

J. L. Harton, T. Hu, M. Krishnamurthy, A. Soffer, W. H. Toki, R. J. Wilson, J. Zhang

Colorado State University, Fort Collins, CO 80523, USA

D. Altenburg, T. Brandt, J. Brose, T. Colberg, M. Dickopp, R. S. Dubitzky, A. Hauke, E. Maly, R. Müller-Pfefferkorn, S. Otto, K. R. Schubert, R. Schwierz, B. Spaan, L. Wilden

Technische Universität Dresden, Institut für Kern- und Teilchenphysik, D-01062 Dresden, Germany

D. Bernard, G. R. Bonneaud, F. Brochard, J. Cohen-Tanugi, S. Ferrag, S. T'Jampens, Ch. Thiebaux, G. Vasileiadis, M. Verderi

Ecole Polytechnique, LLR, F-91128 Palaiseau, France

A. Anjomshoaa, R. Bernet, A. Khan, D. Lavin, F. Muheim, S. Playfer, J. E. Swain, J. Tinslay

University of Edinburgh, Edinburgh EH9 3JZ, United Kingdom

M. Falbo

Elon University, Elon University, NC 27244-2010, USA

C. Borean, C. Bozzi, L. Piemontese, A. Sarti

Università di Ferrara, Dipartimento di Fisica and INFN, I-44100 Ferrara, Italy

E. Treadwell

Florida A&M University, Tallahassee, FL 32307, USA

F. Anulli,[1] R. Baldini-Ferroli, A. Calcaterra, R. de Sangro, D. Falciai, G. Finocchiaro, P. Patteri, I. M. Peruzzi,[1] M. Piccolo, A. Zallo

Laboratori Nazionali di Frascati dell'INFN, I-00044 Frascati, Italy

S. Bagnasco, A. Buzzo, R. Contri, G. Crosetti, M. Lo Vetere, M. Macri, M. R. Monge, S. Passaggio, F. C. Pastore, C. Patrignani, E. Robutti, A. Santroni, S. Tosi

Università di Genova, Dipartimento di Fisica and INFN, I-16146 Genova, Italy

[1] Also with Università di Perugia, I-06100 Perugia, Italy

S. Bailey, M. Morii

Harvard University, Cambridge, MA 02138, USA

R. Bartoldus, G. J. Grenier, U. Mallik

University of Iowa, Iowa City, IA 52242, USA

J. Cochran, H. B. Crawley, J. Lamsa, W. T. Meyer, E. I. Rosenberg, J. Yi

Iowa State University, Ames, IA 50011-3160, USA

M. Davier, G. Grosdidier, A. Höcker, H. M. Lacker, S. Laplace, F. Le Diberder, V. Lepeltier, A. M. Lutz, T. C. Petersen, S. Plaszczynski, M. H. Schune, L. Tantot, S. Trincaz-Duvoid, G. Wormser

Laboratoire de l'Accélérateur Linéaire, F-91898 Orsay, France

R. M. Bionta, V. Brigljević , D. J. Lange, K. van Bibber, D. M. Wright

Lawrence Livermore National Laboratory, Livermore, CA 94550, USA

A. J. Bevan, J. R. Fry, E. Gabathuler, R. Gamet, M. George, M. Kay, D. J. Payne, R. J. Sloane, C. Touramanis

University of Liverpool, Liverpool L69 3BX, United Kingdom

M. L. Aspinwall, D. A. Bowerman, P. D. Dauncey, U. Egede, I. Eschrich, G. W. Morton, J. A. Nash, P. Sanders, D. Smith, G. P. Taylor

University of London, Imperial College, London, SW7 2BW, United Kingdom

J. J. Back, G. Bellodi, P. Dixon, P. F. Harrison, R. J. L. Potter, H. W. Shorthouse, P. Strother, P. B. Vidal

Queen Mary, University of London, E1 4NS, United Kingdom

G. Cowan, H. U. Flaecher, S. George, M. G. Green, A. Kurup, C. E. Marker, T. R. McMahon, S. Ricciardi, F. Salvatore, G. Vaitsas, M. A. Winter

University of London, Royal Holloway and Bedford New College, Egham, Surrey TW20 0EX, United Kingdom

D. Brown, C. L. Davis

University of Louisville, Louisville, KY 40292, USA

J. Allison, R. J. Barlow, A. C. Forti, F. Jackson, G. D. Lafferty, A. J. Lyon, N. Savvas, J. H. Weatherall, J. C. Williams

University of Manchester, Manchester M13 9PL, United Kingdom

A. Farbin, A. Jawahery, V. Lillard, D. A. Roberts, J. R. Schieck

University of Maryland, College Park, MD 20742, USA

G. Blaylock, C. Dallapiccola, K. T. Flood, S. S. Hertzbach, R. Kofler, V. B. Koptchev, T. B. Moore, H. Staengle, S. Willocq

University of Massachusetts, Amherst, MA 01003, USA

B. Brau, R. Cowan, G. Sciolla, F. Taylor, R. K. Yamamoto

Massachusetts Institute of Technology, Laboratory for Nuclear Science, Cambridge, MA 02139, USA

M. Milek, P. M. Patel

McGill University, Montréal, QC, Canada H3A 2T8

F. Palombo

Università di Milano, Dipartimento di Fisica and INFN, I-20133 Milano, Italy

J. M. Bauer, L. Cremaldi, V. Eschenburg, R. Kroeger, J. Reidy, D. A. Sanders, D. J. Summers

University of Mississippi, University, MS 38677, USA

C. Hast, P. Taras

Université de Montréal, Laboratoire René J. A. Lévesque, Montréal, QC, Canada H3C 3J7

H. Nicholson

Mount Holyoke College, South Hadley, MA 01075, USA

C. Cartaro, N. Cavallo, G. De Nardo, F. Fabozzi, C. Gatto, L. Lista, P. Paolucci, D. Piccolo, C. Sciacca

Università di Napoli Federico II, Dipartimento di Scienze Fisiche and INFN, I-80126, Napoli, Italy

J. M. LoSecco

University of Notre Dame, Notre Dame, IN 46556, USA

J. R. G. Alsmiller, T. A. Gabriel

Oak Ridge National Laboratory, Oak Ridge, TN 37831, USA

J. Brau, R. Frey, M. Iwasaki, C. T. Potter, N. B. Sinev, D. Strom, E. Torrence

University of Oregon, Eugene, OR 97403, USA

F. Colecchia, A. Dorigo, F. Galeazzi, M. Margoni, M. Morandin, M. Posocco, M. Rotondo, F. Simonetto, R. Stroili, C. Voci

Università di Padova, Dipartimento di Fisica and INFN, I-35131 Padova, Italy

M. Benayoun, H. Briand, J. Chauveau, P. David, Ch. de la Vaissière, L. Del Buono, O. Hamon, Ph. Leruste, J. Ocariz, M. Pivk, L. Roos, J. Stark

Universités Paris VI et VII, Lab de Physique Nucléaire H. E., F-75252 Paris, France

P. F. Manfredi, V. Re, V. Speziali

Università di Pavia, Dipartimento di Elettronica and INFN, I-27100 Pavia, Italy

L. Gladney, Q. H. Guo, J. Panetta

University of Pennsylvania, Philadelphia, PA 19104, USA

C. Angelini, G. Batignani, S. Bettarini, M. Bondioli, F. Bucci, G. Calderini, E. Campagna, M. Carpinelli, F. Forti, M. A. Giorgi, A. Lusiani, G. Marchiori, F. Martinez-Vidal, M. Morganti, N. Neri, E. Paoloni, M. Rama, G. Rizzo, F. Sandrelli, G. Triggiani, J. Walsh

Università di Pisa, Scuola Normale Superiore and INFN, I-56010 Pisa, Italy

M. Haire, D. Judd, K. Paick, L. Turnbull, D. E. Wagoner

Prairie View A&M University, Prairie View, TX 77446, USA

J. Albert, G. Cavoto,[2] N. Danielson, P. Elmer, C. Lu, V. Miftakov, J. Olsen, S. F. Schaffner, A. J. S. Smith, A. Tumanov, E. W. Varnes

Princeton University, Princeton, NJ 08544, USA

[2] Also with Università di Roma La Sapienza, Roma, Italy

F. Bellini, D. del Re, R. Faccini,[3] F. Ferrarotto, F. Ferroni, E. Leonardi, M. A. Mazzoni, S. Morganti, G. Piredda, F. Safai Tehrani, M. Serra, C. Voena

Università di Roma La Sapienza, Dipartimento di Fisica and INFN, I-00185 Roma, Italy

S. Christ, G. Wagner, R. Waldi

Universität Rostock, D-18051 Rostock, Germany

T. Adye, N. De Groot, B. Franek, N. I. Geddes, G. P. Gopal, S. M. Xella

Rutherford Appleton Laboratory, Chilton, Didcot, Oxon, OX11 0QX, United Kingdom

R. Aleksan, S. Emery, A. Gaidot, P.-F. Giraud, G. Hamel de Monchenault, W. Kozanecki, M. Langer, G. W. London, B. Mayer, G. Schott, B. Serfass, G. Vasseur, Ch. Yeche, M. Zito

DAPNIA, Commissariat à l'Energie Atomique/Saclay, F-91191 Gif-sur-Yvette, France

M. V. Purohit, A. W. Weidemann, F. X. Yumiceva

University of South Carolina, Columbia, SC 29208, USA

I. Adam, D. Aston, N. Berger, A. M. Boyarski, M. R. Convery, D. P. Coupal, D. Dong, J. Dorfan, W. Dunwoodie, R. C. Field, T. Glanzman, S. J. Gowdy, E. Grauges , T. Haas, T. Hadig, V. Halyo, T. Himel, T. Hryn'ova, M. E. Huffer, W. R. Innes, C. P. Jessop, M. H. Kelsey, P. Kim, M. L. Kocian, U. Langenegger, D. W. G. S. Leith, S. Luitz, V. Luth, H. L. Lynch, H. Marsiske, S. Menke, R. Messner, D. R. Muller, C. P. O'Grady, V. E. Ozcan, A. Perazzo, M. Perl, S. Petrak, H. Quinn, B. N. Ratcliff, S. H. Robertson, A. Roodman, A. A. Salnikov, T. Schietinger, R. H. Schindler, J. Schwiening, G. Simi, A. Snyder, A. Soha, S. M. Spanier, J. Stelzer, D. Su, M. K. Sullivan, H. A. Tanaka, J. Va'vra, S. R. Wagner, M. Weaver, A. J. R. Weinstein, W. J. Wisniewski, D. H. Wright, C. C. Young

Stanford Linear Accelerator Center, Stanford, CA 94309, USA

P. R. Burchat, C. H. Cheng, T. I. Meyer, C. Roat

Stanford University, Stanford, CA 94305-4060, USA

R. Henderson

TRIUMF, Vancouver, BC, Canada V6T 2A3

W. Bugg, H. Cohn

University of Tennessee, Knoxville, TN 37996, USA

J. M. Izen, I. Kitayama, X. C. Lou

University of Texas at Dallas, Richardson, TX 75083, USA

F. Bianchi, M. Bona, D. Gamba

Università di Torino, Dipartimento di Fisica Sperimentale and INFN, I-10125 Torino, Italy

L. Bosisio, G. Della Ricca, S. Dittongo, L. Lanceri, P. Poropat, L. Vitale, G. Vuagnin

Università di Trieste, Dipartimento di Fisica and INFN, I-34127 Trieste, Italy

R. S. Panvini

Vanderbilt University, Nashville, TN 37235, USA

[3] Also with University of California at San Diego, La Jolla, CA 92093, USA

S. W. Banerjee, C. M. Brown, D. Fortin, P. D. Jackson, R. Kowalewski, J. M. Roney

University of Victoria, Victoria, BC, Canada V8W 3P6

H. R. Band, S. Dasu, M. Datta, A. M. Eichenbaum, H. Hu, J. R. Johnson, R. Liu, F. Di Lodovico, A. Mohapatra, Y. Pan, R. Prepost, I. J. Scott, S. J. Sekula, J. H. von Wimmersperg-Toeller, J. Wu, S. L. Wu, Z. Yu

University of Wisconsin, Madison, WI 53706, USA

H. Neal

Yale University, New Haven, CT 06511, USA

1 Introduction

The inconsistency between the measured $b \to c\bar{c}s$ rate and the rate of semileptonic B decays has been a long-standing problem in B physics. Until 1994, it was believed that the $b \to c\bar{c}s$ transition was dominated by decays $B \to D_s X$, with some smaller contributions from decays to charmonium states and to charmed strange baryons. Therefore, the branching fraction $b \to c\bar{c}s$ was computed from the inclusive $B \to D_s\, X$, $B \to (c\bar{c})\, X$ and $B \to \Xi_c\, X$ branching fractions, leading to $\mathcal{B}(b \to c\bar{c}s) = (15.8 \pm 2.8)\%$ [1]. Theoretical calculations are unable to simultaneously describe this low branching fraction and the semileptonic branching fraction of the B meson [2].

As a possible explanation of this problem, it has been conjectured [3] that $\mathcal{B}(b \to c\bar{c}s)$ is in fact larger and that decays of the type $B \to \overline{D}^{(*)} D^{(*)} K\,(X)$ (where $D^{(*)}$ can be either a D^0, D^{*0}, D^+ or D^{*+})[1] could contribute significantly to the decay rate. This might also include possible decays to orbitally-excited D_s mesons, $B \to \overline{D}^{(*)} D_s^{**}$, followed by $D_s^{**} \to D^{(*)}\, K$. Experimental evidence in support of this picture has been published in the past few years. This evidence includes the measured branching fraction for wrong-sign D production, averaged over charged and neutral B mesons, by CLEO [4] [$\mathcal{B}(B \to D\, X) = (7.9 \pm 2.2)\%$], and the observation of a small number of fully reconstructed decays $B \to \overline{D}^{(*)} D^{(*)} K$, both by CLEO [5] and ALEPH [6]. More recently, *BABAR* [7] and Belle [8] have released some preliminary conference results on the evidence for transitions $B^0 \to \overline{D}^{(*)0} D^{*+} K^-$ with much larger data sets.

$B \to \overline{D}^{(*)} D^{(*)} K$ decays can occur through two different amplitudes: external W-emission amplitudes and internal W-emission amplitudes (also called color-suppressed amplitudes). Some decays proceed purely through one of these amplitudes while others can proceed through both. Fig. 1 shows the possible types for charged and neutral B decays. In *BABAR*, the large data sets now available allow comprehensive investigations of these transitions. In the analysis described in this note, we present measurements of or limits on the branching fractions for all the possible $B \to \overline{D}^{(*)} D^{(*)} K_S^0$ and $B \to \overline{D}^{(*)} D^{(*)} K^+$ decay modes, using events in which both D mesons are fully reconstructed.

2 The *BABAR* detector and dataset

The study reported here uses $75.9\,\mathrm{fb}^{-1}$ of data collected at the $\Upsilon(4S)$ resonance with the *BABAR* detector, corresponding to $(82.3 \pm 0.9) \times 10^6$ $B\overline{B}$ pairs.

The *BABAR* detector is a large-acceptance solenoidal spectrometer (1.5 T) described in detail elsewhere [9]. The analysis described below makes use of charged track and π^0 reconstruction and charged particle identification. Charged particle trajectories are measured by a 5-layer double-sided silicon vertex tracker (SVT) and a 40-layer drift chamber (DCH), which also provide ionisation measurements ($\mathrm{d}E/\mathrm{d}x$) used for particle identification. Photons and electrons are measured in the electromagnetic calorimeter (EMC), made of 6580 thallium-doped CsI crystals constructed in a non-projective barrel and forward endcap geometry. Charged K/π separation up to $4\,\mathrm{GeV}/c$ in momentum is provided by a detector of internally reflected Cherenkov light (DIRC), consisting of 12 sectors of quartz bars that carry the Cherenkov light to an expansion volume filled with water and equipped with 10751 photomultiplier tubes.

[1] Charge-conjugate reactions are implied throughout this note.

3 B candidate selection

The B^0 and B^+ mesons are reconstructed in a sample of multihadron events for all the possible $\overline{D}DK$ modes, namely $B^0 \to D^{(*)-}D^{(*)0}K^+$, $D^{(*)-}D^{(*)+}K^0$, $\overline{D}^{(*)0}D^{(*)0}K^0$ and $B^+ \to \overline{D}^{(*)0}D^{(*)+}K^0$, $\overline{D}^{(*)0}D^{(*)0}K^+$, $D^{(*)-}D^{(*)+}K^+$. K^0 mesons are reconstructed only from the decays $K^0_S \to \pi^+\pi^-$. To eliminate the background from continuum $e^+e^- \to q\overline{q}$ events, we require that the ratio of the second to zeroth Fox-Wolfram moments [10] be less that 0.45.

The K^0_S candidates are reconstructed from two oppositely charged tracks consistent with coming from a common vertex and having an invariant mass within $\pm 9\,\mathrm{MeV}/c^2$ of the nominal K^0_S mass. For most of the channels involving a K^0_S, we require that the K^0_S vertex is displaced from the interaction point for the event by at least 0.2 cm in the plane transverse to the beam axis direction. The π^0 candidates are reconstructed from pairs of photons, each with an energy greater than 30 MeV, which are required to have a mass $115 < M_{\gamma\gamma} < 150\,\mathrm{MeV}/c^2$. The π^0 from D^{*0} must have a momentum $70 < p^*(\gamma\gamma) < 450\,\mathrm{MeV}/c$ in the $\Upsilon(4S)$ frame, while the π^0 from $D^0 \to K^-\pi^+\pi^0$ must have an energy $E(\pi^0) > 200\,\mathrm{MeV}$.

D^* candidates are reconstructed in the decay modes $D^{*+} \to D^0\pi^+$, $D^{*0} \to D^0\pi^0$ and $D^{*0} \to D^0\gamma$. A $\pm 3\sigma$ interval around the nominal mass difference $\Delta M = M(D^*) - M(D^0)$ is used to select D^* mesons, where σ is the measured mass resolution. For decays $B^0 \to D^{*-}D^{*+}K^0_S$ and $B^+ \to D^{*-}D^{*+}K^+$, one of the $D^{*\pm}$ is also allowed to decay to $D^\pm\pi^0$.

The D^0 and D^+ mesons are reconstructed in the decay modes $D^0 \to K^-\pi^+$, $K^-\pi^+\pi^0$, $K^-\pi^+\pi^-\pi^+$ and $D^+ \to K^-\pi^+\pi^+$, by selecting track combinations with invariant mass within $\pm 2\sigma$ of the average measured D mass. The average D mass and the D mass resolution σ used in this selection are fitted from the data itself, using an inclusive sample of D decays. For modes involving two D^0 mesons, at least one of them is required to decay to $K^-\pi^+$, except for the decay modes $D^{*-}D^{*+}K^0$, $D^{*-}D^{*+}K^+$ and $D^{*-}D^0K^+$, which have lower background. The K and π tracks are required to be well reconstructed in the tracking detectors and to originate from a common vertex. Charged kaon identification, based on the measured Cherenkov angle in the DIRC and the $\mathrm{d}E/\mathrm{d}x$ measurements in the drift chamber and the vertex tracker, is used for most D decay modes, as well as for the K^+ from the B meson decay.

B candidates are reconstructed from one $\overline{D}^{(*)}$, one $D^{(*)}$ and one K candidate. A mass constraint is applied to all the intermediate particles (D^{*0}, D^{*+}, D^0, D^+, K^0_S, π^0). Since the B mesons are produced via $e^+e^- \to \Upsilon(4S) \to B\overline{B}$, the energy of the B in the $\Upsilon(4S)$ frame is given by the beam energy E^*_{beam}, which is known much more precisely than the energy of the B candidate. Therefore, to isolate the B meson signal, we use two kinematic variables: ΔE, the difference between the reconstructed energy of the B candidate and the beam energy in the center of mass frame, and m_{ES}, the beam energy substituted mass, defined as

$$m_{\mathrm{ES}} = \sqrt{E^{*2}_{beam} - p^{*2}_B}, \tag{1}$$

where p^*_B is the momentum of the reconstructed B in the $\Upsilon(4S)$ frame. Signal events have ΔE close to 0 and m_{ES} close to the B meson mass, $5.729\,\mathrm{GeV}/c^2$. When several candidates are selected in an event, only the candidate with the lowest $|\Delta E|$ value is considered ("best candidate"). From Monte Carlo studies, this algorithm is found to give the best reconstruction efficiency and the lower cross-feed between the different $\overline{D}^{(*)}D^{(*)}K$ modes; it is found to introduce no bias on the signal extraction, since the latter is performed from the m_{ES} spectra only. However, in the Fig. 2, to avoid the bias on ΔE inherent to the method, all the ΔE spectra are shown without this requirement.

4 Evidence for a signal in the sum of all B submodes

The $m_{\rm ES}$ and ΔE spectra of the selected events are shown in Fig. 2 for the sum of all the decay modes, separately for B^0 and B^+. The ΔE spectra are shown for events in the signal region defined by $5.27 < m_{\rm ES} < 5.29\,{\rm GeV}/c^2$. Signal events appear in the peak near 0 MeV when reconstructed correctly, while the peak around -160 MeV is due to $\overline{D}^* DK$ or $\overline{D}^* D^* K$ decays reconstructed as $\overline{D}DK$ or $\overline{D}^* DK$, respectively. The $m_{\rm ES}$ spectra for the signal region are shown for events with ΔE within $\pm 2.5\sigma_{\Delta E}$ of the central ΔE value for the signal. The resolution $\sigma_{\Delta E}$ is determined from the data and is equal to 9.9 MeV for events involving no D^{*0} and 11.3 MeV for events involving one D^{*0}. For events with two D^{*0}, the resolution is estimated from the Monte Carlo simulation to be 13.8 MeV. A shift $\Delta E_{\rm shift} = (-5 \pm 1)$ MeV of the ΔE central value for the signal is observed in the data. This shift is due to imperfect modeling of the charged K energy losses in the detector material and is accounted for in the analysis. As explained above, only the candidate with the lowest $|\Delta E - \Delta E_{\rm shift}|$ appears in the $m_{\rm ES}$ spectra in case of multiple candidates. Both the $m_{\rm ES}$ spectra for the ΔE signal region and the ΔE spectra show clear evidence of a signal. On the contrary, the $m_{\rm ES}$ spectra for the background control region $\Delta E > 50$ MeV show no evidence of any excess of events in the B signal region. For the $m_{\rm ES}$ spectra, the combinatorial background is empirically described by the ARGUS function [11]

$$\frac{dN}{dm_{\rm ES}} = f(m_{\rm ES}; A, \zeta) = A \times m_{\rm ES} \times \sqrt{1 - \frac{m_{\rm ES}^2}{E_{beam}^{*2}}} \times \exp\left[-\zeta \left(1 - \frac{m_{\rm ES}^2}{E_{beam}^{*2}}\right)\right], \qquad (2)$$

where A is a normalisation factor. The function depends on a free parameter ζ that is determined from a fit to the $m_{\rm ES}$ spectra of the background control region. The number of combinatorial background events in the signal region is then estimated by normalizing the ARGUS function to the region $5.22 < m_{\rm ES} < 5.27\,{\rm GeV}/c^2$ in the projection containing the signal (Fig. 2c,d) and extrapolating it to the signal region $5.27 < m_{\rm ES} < 5.29\,{\rm GeV}/c^2$. The fitted ARGUS functions are overlaid on the $m_{\rm ES}$ spectra of Fig. 2. The average number of background events expected in the signal region is 1889±24 for neutral B mesons and 2512±27 for charged B mesons, while 2712 and 3482 events are observed, giving an excess of 823±57 B^0 and 969±65 B^+ events in the signal region.

5 Measurement of exclusive branching fractions

In the following, the subscript k will be used to identify the different $B \to \overline{D}^{(*)} D^{(*)} K$ decay modes (i.e., $\overline{D}^0 D^0 K^+$, $D^{*-} D^0 K^+$, ...). The subscript i will be used to identify the different decay submodes of the $\overline{D}D$ pair (i.e., $i = K\pi \times K\pi$, $K\pi \times K\pi\pi^0$, $K\pi \times K3\pi$, ...). The subscript ik will therefore refer to the B mode k decaying into the $\overline{D}D$ submode i.

The $m_{\rm ES}$ spectra obtained after a $\pm 2.5\sigma_{\Delta E}$ selection on $(\Delta E - \Delta E_{\rm shift})$ for all the different $\overline{D}^{(*)} D^{(*)} K$ modes are shown in Fig. 3 (B^0 decay modes) and Fig. 4 (B^+ decay modes). The corresponding event yields, computed as explained below, are given in Table 1. In Figs. 3 and 4 and in Table 1, for a given B decay mode the signals from the different $\overline{D}D$ decay submodes have been summed. However, to take advantage of the different signal-to-background ratio of the various submodes, the information from each submode is entered separately in a likelihood function used to calculate the $B \to \overline{D}^{(*)} D^{(*)} K$ branching fractions. As a first step, the ARGUS shape parameter of each submode, ζ_{ik}, is determined from a fit to the $m_{\rm ES}$ spectra of the background control region

$\Delta E > 50\,\mathrm{MeV}$. An ARGUS function with the shape parameter ζ fixed to this value is then fitted to the $m_{\rm ES}$ distribution for the signal region $|\Delta E - \Delta E_{\rm shift}| < 2.5\sigma_{\Delta E}$, excluding from the fit events with $5.27 < m_{\rm ES} < 5.29\,\mathrm{GeV}/c^2$. A value for the background normalization parameter A_{ik} is calculated and the number of background events $N_{ik}^{\rm bkg}$ in the signal region for this submode is calculated as

$$N_{ik}^{\rm bkg} = \int_{5.27}^{5.29} f\left(x; A_{ik}, \zeta_{ik}\right) dx. \tag{3}$$

If n_k submodes are used for a given mode, the branching fraction for that mode is then extracted by maximizing the following likelihood:

$$L_k = \prod_{i=1}^{n_k} \frac{{\mu_{ik}}^{N_{ik}} e^{-\mu_{ik}}}{N_{ik}!}, \tag{4}$$

where N_{ik} is the observed number of events in the signal region and μ_{ik} is the predicted number of events in the signal region. μ_{ik} is the sum of three contributions:

- the predicted signal N_{ik}^S, which is related to the (unknown) branching fraction $\mathcal{B}_k$ of decay mode k, the reconstruction efficiency (ϵ_{ik}), the intermediate branching fractions $\mathcal{B}_i^{\overline{D}D}$ and the number of $B\overline{B}$ events ($N_{B\overline{B}}$)

$$N_{ik}^S = \mathcal{B}_k \times N_{B\overline{B}} \times \epsilon_{ik} \times \mathcal{B}_i^{\overline{D}D}; \tag{5}$$

- the number of combinatorial background events $N_{ik}^{\rm bkg}$, determined as described above (Eq.3);

- the peaking background $N_{ik}^{\rm peak}$ from other $B \to \overline{D}^{(*)} D^{(*)} K$ decay modes, calculated as

$$N_{ik}^{\rm peak} = \sum_{l \neq k} \mathcal{B}_l \times N_{B\overline{B}} \times \epsilon'(il \to ik) \times \mathcal{B}_i^{\overline{D}D}, \tag{6}$$

  where $\epsilon'(il \to ik)$ is the cross-feed matrix from B mode l to B mode k for the $\overline{D}D$ decay submodes i (the cross-feed between different $\overline{D}D$ decay submodes is found to be negligible). The only significant cross-feed is observed between decay modes where a fake D^{*0} replaces a true D^{*+} or a true D^0, for instance between $D^{*-}D^0K^+$ and $\overline{D}^{*0}D^0K^+$, or between $\overline{D}^{*0}D^0K^+$ and $\overline{D}^0 D^{*0} K^+$. Therefore, these branching fractions are extracted with joint likelihood in Eq. 4.

The D^* and D branching fractions used in the branching fraction calculation are summarized in Table 2 [12]. The selection efficiencies and the cross-feed matrices for each mode are obtained from a detailed Monte Carlo simulation, in which the detector response is modeled with the GEANT4 program. B meson decays to $\overline{D}DK$ are generated with a three-body phase space model in the simulated event samples used for the efficiency calculation. For each decay submode, samples of about 15000 signal events have been produced. In addition, data are used whenever possible to determine detector performance: tracking efficiencies are determined by identifying tracks in the silicon vertex detector and measuring the fraction that is well reconstructed in the drift chamber; the kaon identification efficiency is estimated from a sample of $D^{*+} \to D^0\pi^+$, $D^0 \to K^-\pi^+$ decays; the γ and π^0 efficiencies are measured by comparing the ratio of events $N(\tau^+ \to \overline{\nu}_\tau h^+\pi^0)/N(\tau^+ \to \overline{\nu}_\tau h^+\pi^0\pi^0)$ to the previously measured branching fractions [13]. Typical efficiencies range from 20%, for $B^0 \to \overline{D}^0 D^0 K^+$ with both D^0 mesons decaying to $K^-\pi^+$, to less than 1%, for $B^+ \to D^{*-}D^{*+}K^+$ ($D^{*+} \to D^0\pi^+$, $D^{*-} \to \overline{D}^0\pi^-$) with D^0 mesons decaying to $K^-\pi^+\pi^0$ or $K^-\pi^+\pi^-\pi^+$.

Table 1: Number of events and branching fractions for each mode. The first error on the branching fraction is the statistical uncertainty and the second one is the systematic uncertainty.

B decay mode	Total yield in signal region	Estimated background	Excess	Branching fraction (10^{-3})	90% C.L. upper limit (10^{-3})
B^0 decays through external W-emission amplitudes					
$B^0 \to D^- D^0 K^+$	599	479±12	120±27	$1.7 \pm 0.3 \pm 0.3$	
$B^0 \to D^- D^{*0} K^+$	468	337±10	131±24	$4.6 \pm 0.7 \pm 0.7$	
$B^0 \to D^{*-} D^0 K^+$	584	399±11	185±27	$3.1^{+0.4}_{-0.3} \pm 0.4$	
$B^0 \to D^{*-} D^{*0} K^+$	289	84±5	205±18	$11.8 \pm 1.0 \pm 1.7$	
B^0 decays through external+internal W-emission amplitudes					
$B^0 \to D^- D^+ K^0$	26	19±2	7±5	$0.8^{+0.6}_{-0.5} \pm 0.3$	< 1.7
$B^0 \to D^{*-} D^+ K^0$+CC	84	34±3	50±10	$6.5 \pm 1.2 \pm 1.0$	
$B^0 \to D^{*-} D^{*+} K^0$	116	48±4	68±11	$8.8^{+1.5}_{-1.4} \pm 1.3$	
B^0 decays through internal W-emission amplitudes					
$B^0 \to \overline{D}^0 D^0 K^0$	175	173±7	2±15	$0.8 \pm 0.4 \pm 0.2$	< 1.4
$B^0 \to \overline{D}^0 D^{*0} K^0$+CC	248	225±8	23±18	$1.7^{+1.4}_{-1.3} \pm 0.7$	< 3.7
$B^0 \to \overline{D}^{*0} D^{*0} K^0$	123	81±6	42±13	$3.3^{+2.1}_{-2.0} \pm 1.4$	< 6.6
B^+ decays through external W-emission amplitudes					
$B^+ \to \overline{D}^0 D^+ K^0$	367	317±9	50±21	$1.8 \pm 0.7 \pm 0.4$	< 2.8
$B^+ \to \overline{D}^{*0} D^+ K^0$	216	175±7	41±16	$4.1^{+1.5}_{-1.4} \pm 0.8$	< 6.1
$B^+ \to \overline{D}^0 D^{*+} K^0$	77	31±3	46±9	$5.2^{+1.0}_{-0.9} \pm 0.7$	
$B^+ \to \overline{D}^{*0} D^{*+} K^0$	89	43±4	46±10	$7.8^{+2.3}_{-2.1} \pm 1.4$	
B^+ decays through external+internal W-emission amplitudes					
$B^+ \to \overline{D}^0 D^0 K^+$	627	469±11	158±27	$1.9 \pm 0.3 \pm 0.3$	
$B^+ \to \overline{D}^{*0} D^0 K^+$	552	411±11	141±26	$1.8^{+0.7}_{-0.6} \pm 0.4$	< 3.8
$B^+ \to \overline{D}^0 D^{*0} K^+$	623	402±11	221±27	$4.7 \pm 0.7 \pm 0.7$	
$B^+ \to \overline{D}^{*0} D^{*0} K^+$	675	468±15	207±30	$5.3^{+1.1}_{-1.0} \pm 1.2$	
B^+ decays through internal W-emission amplitudes					
$B^+ \to D^- D^+ K^+$	64	65±4	-1±9	$0.0 \pm 0.3 \pm 0.1$	< 0.4
$B^+ \to D^- D^{*+} K^+$	45	39±4	6±8	$0.2 \pm 0.2 \pm 0.1$	< 0.7
$B^+ \to D^{*-} D^+ K^+$	64	32±3	32±9	$1.5 \pm 0.3 \pm 0.2$	
$B^+ \to D^{*-} D^{*+} K^+$	83	60±4	23±10	$0.9 \pm 0.4 \pm 0.2$	< 1.8

6 Systematic studies

Due to the large number of $K^\pm$ and to the large multiplicities involved in the decays $B \to \overline{D}^{(*)} D^{(*)} K$, the dominant systematic uncertainties come from our level of understanding of the charged kaon identification and of the charged particle tracking efficiencies. Both systematic uncertainties are estimated on a per track basis and are given in Table 3. Other systematic uncertainties are due to uncertainties on the D and D^* branching fractions, the π^0 reconstruction efficiencies, the D vertexing requirements, and the ΔE resolution used to define the signal box, as well as the

Table 2: Submode branching fractions used in the analysis [12]. The errors on the $\mathcal{B}(D^0 \to K^-\pi^+\pi^0)$ and $\mathcal{B}(D^0 \to K^-\pi^+\pi^-\pi^+)$ correlated to the error on $\mathcal{B}(D^0 \to K^-\pi^+)$ are indicated separately with the subscript $K\pi$.

Mode	$\mathcal{B}$ (%)
$D^0 \to K^-\pi^+$	3.80 ± 0.09
$D^0 \to K^-\pi^+\pi^0$	$13.10 \pm 0.84 \pm 0.31_{K\pi}$
$D^0 \to K^-\pi^+\pi^-\pi^+$	$7.46 \pm 0.30 \pm 0.18_{K\pi}$
$D^+ \to K^-\pi^+\pi^+$	9.1 ± 0.6
$D^{*+} \to D^0\pi^+$	67.7 ± 0.5
$D^{*+} \to D^+\pi^0$	30.7 ± 0.5
$D^{*0} \to D^0\pi^0$	61.9 ± 2.9
$D^{*0} \to D^0\gamma$	38.1 ± 2.9
$K^0_S \to \pi^+\pi^-$	68.61 ± 0.28

uncertainty on the combinatorial background estimates, the statistical uncertainty on the efficiency due to the finite size of the Monte Carlo simulation samples and the uncertainty on the number of $B\overline{B}$ events in the data sample. The fractional systematic uncertainties on efficiencies and the branching fractions are summarized in Table 3.

Possible decay model dependence of the efficiencies were also studied by generating decays $B^0 \to D^{*-}D^+_{s1}$ and $B^0 \to D^{*-}D'^+_{s1}$ ($D^+_{s1}, D'^+_{s1} \to D^{*0}K^+$), where D^+_{s1} is the narrow ($\Gamma = 1\,\mathrm{MeV}$, $M = 2.536\,\mathrm{GeV}/c^2$) orbitally excited 1^+ state of the D^{**}_s system and D'^+_{s1} is a wide ($\Gamma = 250\,\mathrm{MeV}$, $M = 2.560\,\mathrm{GeV}/c^2$) D^{**}_s resonance. The efficiency for reconstructing these modes was compared to the efficiency found for decays $B^0 \to D^{*-}D^{*0}K^+$ generated with a phase space model. We found no statistically significant difference in efficiencies; we assign a systematic uncertainty equal to the statistical error of 5%.

7 Conclusions

A preliminary measurement of the branching fractions for the 22 $B \to \overline{D}^{(*)}D^{(*)}K$ modes is given in Table 1. For the channels for which $\mathrm{S}/\sqrt{\mathrm{B}}$ is smaller than 4, a 90% confidence level upper limit is also derived. (Here, B is the sum of the combinatorial background and of the cross-feed background from other $\overline{D}^{(*)}D^{(*)}K$ modes and $\mathrm{S} = \mathrm{N} - \mathrm{B}$, where N is the total yield in the signal region). This is the first time that a complete measurement of all the possible $B \to \overline{D}^{(*)}D^{(*)}K$ channels is performed. The measured branching fractions are in good agreement with earlier measurements made with smaller data sets for some of these modes [5, 6, 7, 8]. For the decays proceeding through external W-emission or through the sum of external and internal W-emission amplitudes, the branching fractions $\mathcal{B}(B \to \overline{D}^*DK)$ and $\mathcal{B}(B \to \overline{D}D^*K)$ are found to be about twice the branching fraction $\mathcal{B}(B \to \overline{D}DK)$. The branching fraction $\mathcal{B}(B \to \overline{D}^*D^*K)$ is found to be about 5 times larger than the branching fraction $\mathcal{B}(B \to \overline{D}DK)$. No significant difference is observed between decays proceeding through external spectator amplitudes and decays proceeding through the sum of external and internal spectator amplitudes.

After summing over all submodes, the preliminary branching fractions of the B^0 and of the B^+

Table 3: Fractional systematic uncertainties on efficiencies and branching fractions.

Item	Fractional uncertainty on efficiency or branching fraction
Charged tracks reconstruction	0.8% per track for good tracks in Drift Chamber 1.2% per track for tracks without Drift Chamber requirements
K^0_S reconstruction	2.5% per K^0_S, added in quadrature to the track reconstruction error
π^0 reconstruction	5.1% per π^0
γ from $D^{*0} \to D^0\gamma$	5.1% per γ (correlated with the π^0 systematic)
$K^\pm$ identification	2.5% per $K^\pm$
Vertex reconstruction	1.3% per 2 track vertex 3.1% per 3 track vertex 5.7% per 4 track vertex
$\sigma(\Delta E)$	2% for modes with 0 or 1 D^{*0} 5% for modes with two D^{*0}'s
Monte Carlo statistics	2% to 10% per $\overline{D}D$ submode (mode and submode dependent)
Intermediate br. fraction	see Table 2
Number of $B\overline{B}$	1.1%
Decay model	5%

to $\overline{D}^{(*)}D^{(*)}K$ are found to be

$$\mathcal{B}(B^0 \to \overline{D}^{(*)}D^{(*)}K) = (4.3 \pm 0.3(stat) \pm 0.6(syst)) \times 10^{-2}, \quad (7)$$

$$\mathcal{B}(B^+ \to \overline{D}^{(*)}D^{(*)}K) = (3.5 \pm 0.3(stat) \pm 0.5(syst)) \times 10^{-2}. \quad (8)$$

This study confirms that a significant fraction of the transitions $b \to c\overline{c}s$ proceeds through the decays $B \to \overline{D}^{(*)}D^{(*)}K$. These decay modes account for about one half of the wrong-sign D production rate in B decays, $\mathcal{B}(B \to D\,X) = (7.9 \pm 2.2)\%$ [4]; however, because of the large statistical error on the latter measurement, it is not yet clear whether they saturate it.

Future developments should include a search for D^{**}_s resonant substructures in $B \to \overline{D}^{(*)}D^{(*)}K$ decays, as well as a new high statistics measurement of the wrong sign D production in B decays and a search for decays $B \to \overline{D}^{(*)}D^{(*)}K^*$ or $B \to \overline{D}^{(*)}D^{(*)}K(n\pi)$.

8 Acknowledgments

We are grateful for the extraordinary contributions of our PEP-II colleagues in achieving the excellent luminosity and machine conditions that have made this work possible. The success of this project also relies critically on the expertise and dedication of the computing organizations that support *BABAR*. The collaborating institutions wish to thank SLAC for its support and the kind hospitality extended to them. This work is supported by the US Department of Energy and National Science Foundation, the Natural Sciences and Engineering Research Council (Canada), Institute of High Energy Physics (China), the Commissariat à l'Energie Atomique and Institut National de Physique Nucléaire et de Physique des Particules (France), the Bundesministerium für Bildung

und Forschung and Deutsche Forschungsgemeinschaft (Germany), the Istituto Nazionale di Fisica Nucleare (Italy), the Research Council of Norway, the Ministry of Science and Technology of the Russian Federation, and the Particle Physics and Astronomy Research Council (United Kingdom). Individuals have received support from the A. P. Sloan Foundation, the Research Corporation, and the Alexander von Humboldt Foundation.

References

[1] T. Browder, Proceedings of the 1996 Warsaw conference, Z. Ajduk and A.K. Wroblewski Eds., World Scientific (1997) p. 1139.

[2] I. I. Bigi, B. Blok, M. Shifman, and A. Vainshtein, Phys. Lett. **B323**, 408 (1994).

[3] G. Buchalla, I. Dunietz, and H. Yamamoto, Phys. Lett. **B364**, 188 (1995).

[4] CLEO Collaboration, T. E. Coan *et al.*, Phys. Rev. Lett. **80**, 1150 (1998).

[5] CLEO Collaboration, CLEO CONF 97-26, EPS97 337.

[6] ALEPH Collaboration, R. Barate *et al.*, Eur. Phys. J. **C4**, 387 (1998).

[7] *BABAR* Collaboration, B. Aubert *et al.*, SLAC-PUB-8924, hep-ex/0107056.

[8] Belle Collaboration, K. Abe *et al.*, BELLE-CONF-0104.

[9] *BABAR* Collaboration, B. Aubert *et al.*, Nucl. Instrum. Methods **A479**, 1 (2002).

[10] G.C. Fox and S. Wolfram, Nucl. Phys. **B149**, 413 (1979).

[11] ARGUS Collaboration, H. Albrecht *et al.*, Phys. Lett. **B241**, 278 (1990).

[12] Particle Data Group, K. Hagiwara *et al.*, Phys. Rev. **D66**, 010001 (2002).

[13] CLEO Collaboration, M. Procario *et al.*, Phys. Rev. Lett. **70**, 1207 (1993).

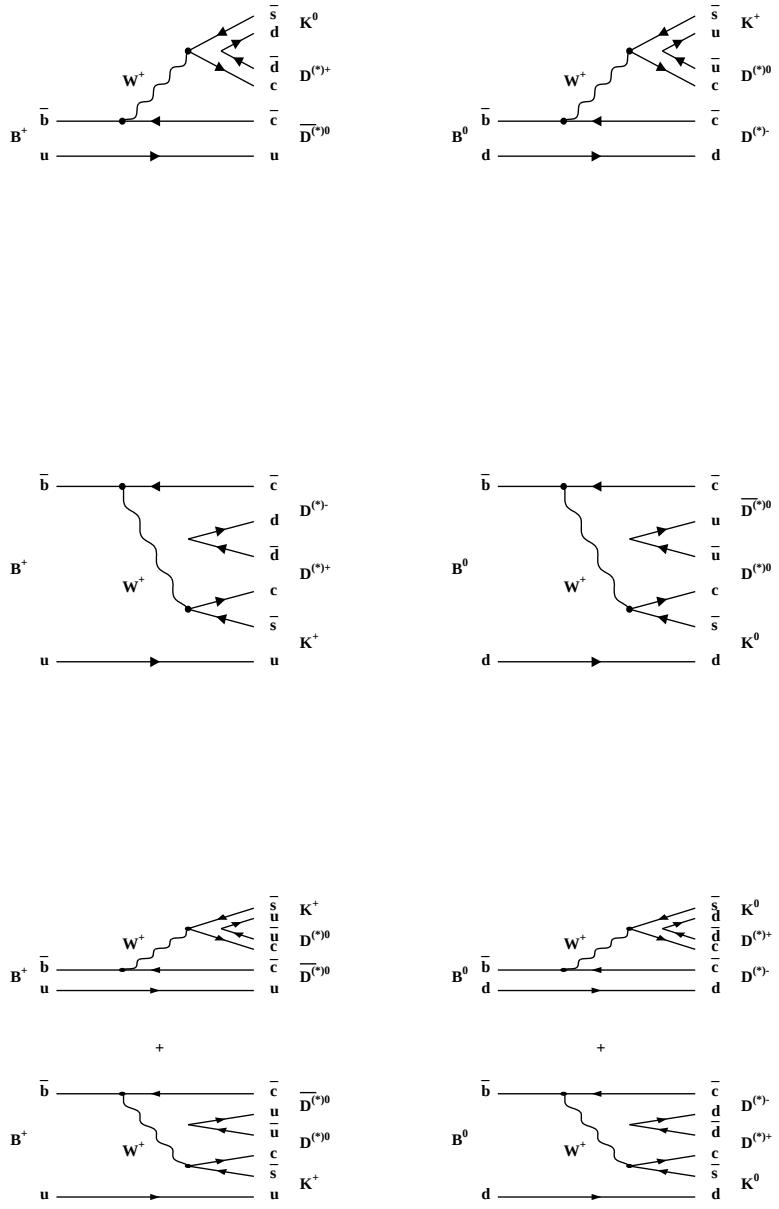

Figure 1: Top row: external W-emission amplitudes for the decays $B^+ \to \overline{D}^{(*)0} D^{(*)+} K^0$ and $B^0 \to D^{(*)-} D^{(*)0} K^+$. Second row: internal W-emission amplitudes for the decays $B^+ \to D^{(*)-} D^{(*)+} K^+$ and $B^0 \to \overline{D}^{(*)0} D^{(*)0} K^0$. Bottom rows: external+internal W-emission amplitudes for the decays $B^+ \to \overline{D}^{(*)0} D^{(*)0} K^+$ and $B^0 \to D^{(*)-} D^{(*)+} K^0$.

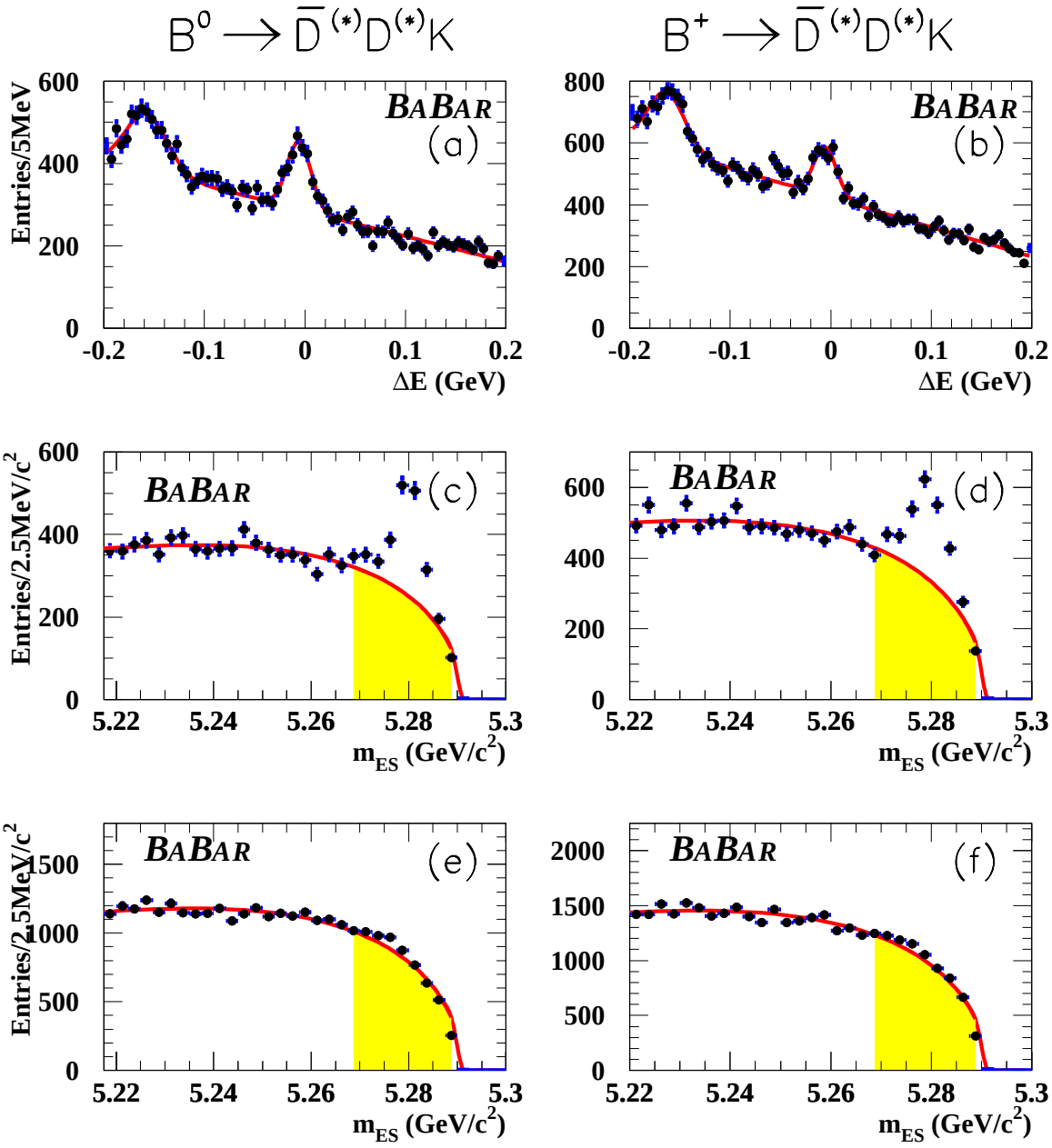

Figure 2: The ΔE and $m_{\rm ES}$ spectra (a,c,e) for the sum of all the $B^0 \to \overline{D}^{(*)}D^{(*)}K$ modes and (b,d,f) for the sum of all the $B^+ \to \overline{D}^{(*)}D^{(*)}K$ modes. (a,b): ΔE for $m_{\rm ES} > 5.27\,{\rm GeV}/c^2$. (c,d): $m_{\rm ES}$ for $\Delta E < 2.5\sigma$ (signal box). (e,f): $m_{\rm ES}$ for $\Delta E > 50\,{\rm MeV}$ (background control region). The curves superimposed to the $m_{\rm ES}$ spectra correspond to the ARGUS background fits described in the text and the shaded regions represent the background under the signal region $5.27 < m_{\rm ES} < 5.29\,{\rm GeV}/c^2$.

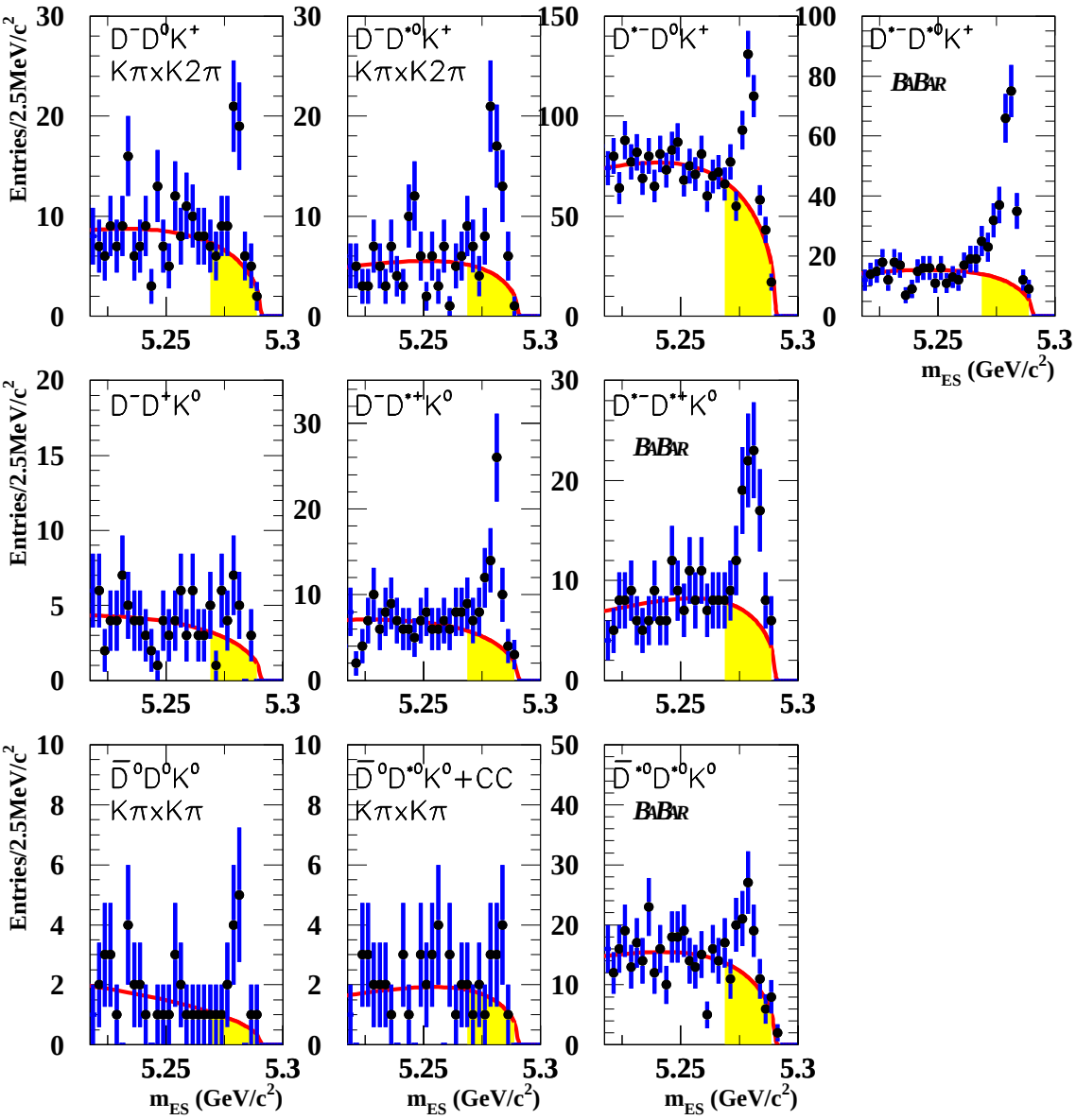

Figure 3: The $m_{\rm ES}$ spectra of the ten $B^0 \to \overline{D}^{(*)} D^{(*)} K$ modes. For each mode, all the D decay submodes used in the analysis have been summed, except for plots where the $\bar{D} \times D$ decay modes used appear explicitly. The curves correspond to the background fits described in the text and the shaded regions represent the background under the signal box. Upper row: pure external spectator $B^0 \to D^{(*)-} D^{(*)0} K^+$ decays. Middle row: external+internal decays $B^0 \to D^{(*)-} D^{(*)+} K^0_S$. Bottom row: pure internal (color suppressed) decays $B^0 \to \overline{D}^{(*)0} D^{(*)0} K^0_S$.

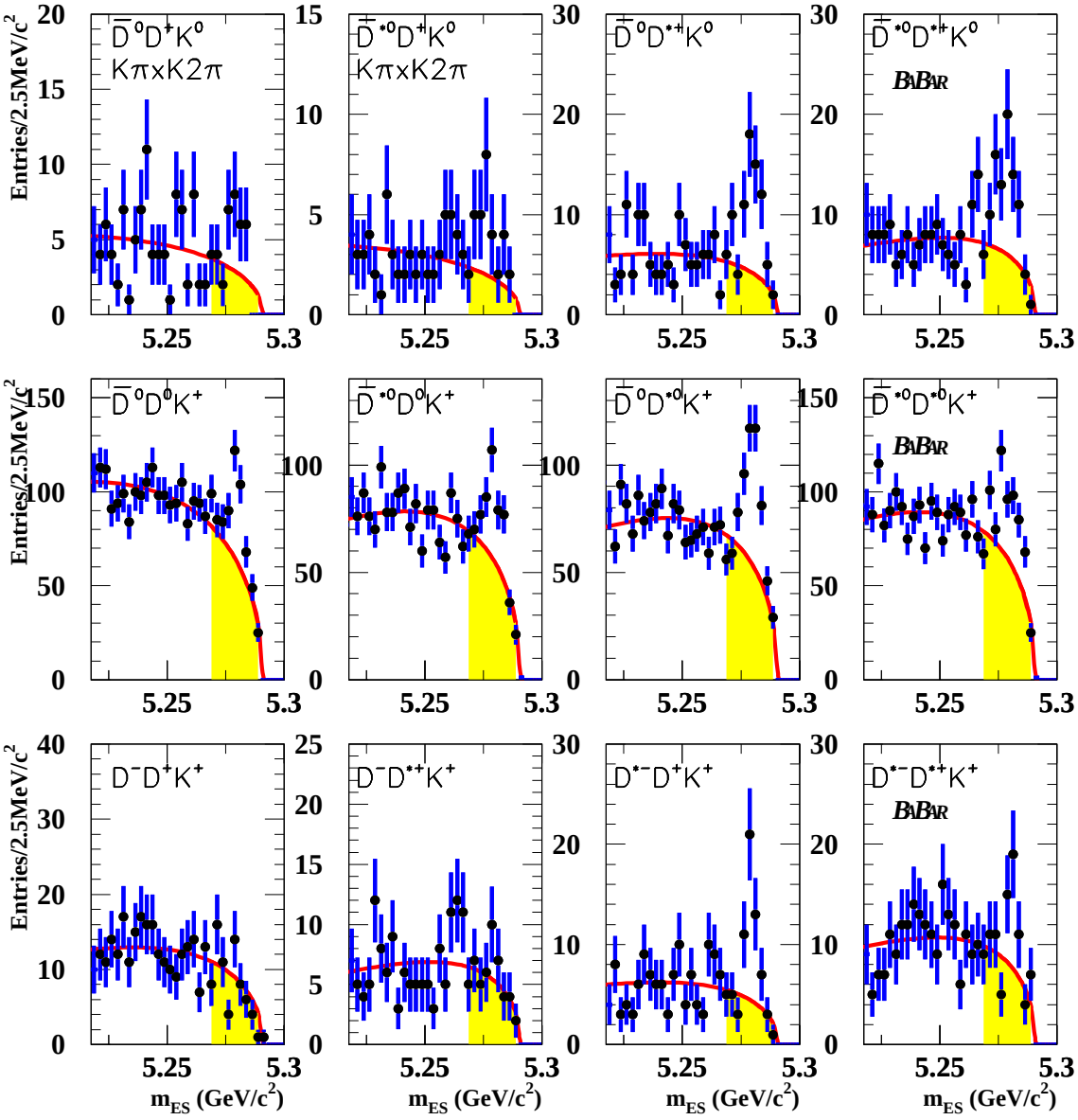

Figure 4: The $m_{\rm ES}$ spectra of the twelve $B^+ \to \overline{D}^{(*)} D^{(*)} K$ modes. For each mode, all the D decay submodes used in the analysis have been summed, except for plots where the $\bar{D} \times D$ decay modes used appear explicitly. The curves correspond to the background fits described in the text and the shaded regions represent the background under the signal box. Upper row: pure external spectator decays $B^+ \to \overline{D}^{(*)0} D^{(*)+} K^0_S$. Middle row: external+internal decays $B^+ \to \overline{D}^{(*)0} D^{(*)0} K^+$. Bottom row: pure internal (color suppressed) decays $B^+ \to D^{(*)-} D^{(*)+} K^+$.